

Enhanced Low-Complexity FDD System Feedback with Variable Bit Lengths via Generative Modeling

Nurettin Turan, Benedikt Fesl, and Wolfgang Utschick

School of Computation, Information and Technology, Technical University of Munich, Germany

Email: {nurettin.turan, benedikt.fesl, utschick}@tum.de

Abstract—Recently, a versatile limited feedback scheme based on a Gaussian mixture model (GMM) was proposed for frequency division duplex (FDD) systems. This scheme provides high flexibility regarding various system parameters and is applicable to both point-to-point multiple-input multiple-output (MIMO) and multi-user MIMO (MU-MIMO) communications. The GMM is learned to cover the operation of all mobile terminals (MTs) located inside the base station (BS) cell, and each MT only needs to evaluate its strongest mixture component as feedback, eliminating the need for channel estimation at the MT. In this work, we extend the GMM-based feedback scheme to variable feedback lengths by leveraging a single learned GMM through merging or pruning of dispensable mixture components. Additionally, the GMM covariances are restricted to Toeplitz or circulant structure through model-based insights. These extensions significantly reduce the offloading amount and enhance the clustering ability of the GMM which, in turn, leads to an improved system performance. Simulation results for both point-to-point and multi-user systems demonstrate the effectiveness of the proposed extensions.

Index Terms—Gaussian mixture models, machine learning, limited feedback, precoding, frequency division duplexing.

I. INTRODUCTION

In the next generation of cellular systems (6G), the BS has the ability to adjust to changing channel conditions. However, in FDD systems, this adaptation must rely on feedback from the MT since channel reciprocity is not maintained [1]. There is considerable interest in systems that use limited feedback, where only a few bits are designated [1]. In this context, two main strategies can be distinguished. The first involves estimating the downlink (DL) channel at the MTs and determining the feedback based on this [1]–[3]. The second approach aims to directly encode feedback from pilot observations, such as through deep learning, cf., e.g., [4], [5].

In recent works, a versatile GMM-based limited feedback scheme was proposed which provides flexibility with respect to the number of antennas, the transmission mode, the supported signal-to-noise ratio (SNR) range, the number of pilots, and the choice of the precoding algorithm, together with low complexity to determine the feedback by entirely circumventing the necessity for channel estimation at the MT [6], [7]. The corresponding GMM is learned from data which represent

The authors acknowledge the financial support by the Federal Ministry of Education and Research of Germany in the program of “Souverän. Digital. Vernetzt.”. Joint project 6G-life, project identification number: 16KISK002.

©This work has been submitted to the IEEE for possible publication. Copyright may be transferred without notice, after which this version may no longer be accessible.

the underlying channel distribution of a whole communication scenario inside a BS cell. This is motivated by the universal approximation property [8] and the strong results of GMMs in wireless communications [9]–[12]. A main advantage is that the offline fitting of the GMM can be done centralized at the BS due to the absence of a distributional shift between the channel distributions of uplink (UL) and DL, cf. [13]–[15].

Although GMMs possess the universal approximation property, cf. [8], a known trait is that their corresponding mixture components may not be distinct enough from each other to be interpreted as clusters [16]. This similarly also arises in the GMM-based feedback scheme from [7], where the number K of mixture components is predetermined by the number B of feedback bits, i.e., $K = 2^B$. Therefore, the GMM should exhibit both a strong clustering ability for selecting the feedback index and a good likelihood model for the underlying channel distribution of the communication scenario, while maintaining a fixed number of components. To address this problem, various merging and pruning techniques have been proposed in the literature [16], [17]. Furthermore, structural features of the covariance matrices, imposed by the antenna arrays, can be utilized in order to reduce the number of parameters of the GMM which, in turn, leads to a higher robustness against overfitting for a limited amount of training data [11].

Contributions: This work extends the versatile GMM-based feedback scheme from [6], [7] by leveraging a single learned GMM to variable feedback bit lengths through merging or pruning of dispensable mixture components. Thereby, a simple pruning technique and a merging approach—which combines components with high similarity—is analyzed. Additionally, we investigate the restriction of the GMM to Toeplitz- and circulant-structured covariances which drastically reduces the necessary offloading overhead from the BS to the MTs and prevents overfitting in the case of limited training data. Simulation results show that the reduction of GMM components through merging or pruning enables variable bit lengths and is superior to directly fitting a smaller GMM because of the enhanced clustering ability. Furthermore, the structured GMM variants yield great performances with low memory overhead for both point-to-point and MU-MIMO systems.

II. SYSTEM AND CHANNEL MODELS

A. Data Transmission – Point-to-Point MIMO System

The DL received signal of a point-to-point MIMO system can be expressed as $\mathbf{y}' = \mathbf{H}\mathbf{x} + \mathbf{n}'$, where $\mathbf{y}' \in \mathbb{C}^{N_{\text{rx}}}$ is the receive vector, $\mathbf{x} \in \mathbb{C}^{N_{\text{tx}}}$ is the transmit vector sent over the MIMO channel $\mathbf{H} \in \mathbb{C}^{N_{\text{rx}} \times N_{\text{tx}}}$, and $\mathbf{n}' \sim \mathcal{N}_{\mathbb{C}}(\mathbf{0}, \sigma_n^2 \mathbf{I}_{N_{\text{rx}}})$ denotes the additive white Gaussian noise (AWGN). In this paper, we consider configurations with $N_{\text{rx}} < N_{\text{tx}}$. The feedback consists of B bits, which are commonly used for encoding an index $k^* \in \{1, 2, \dots, 2^B\}$ that specifies an element from a set of 2^B pre-computed transmit covariance matrices $\mathcal{Q} = \{\mathbf{Q}_1, \mathbf{Q}_2, \dots, \mathbf{Q}_{2^B}\}$ [1].

B. Data Transmission – Multi-user MIMO System

We adopt linear precoding in a single-cell MU-MIMO DL system. The BS is equipped with N_{tx} transmit antennas and each MT $j \in \mathcal{J} = \{1, 2, \dots, J\}$, is equipped with N_{rx} antennas. The precoded DL data vector is $\mathbf{x} = \sum_{j=1}^J \mathbf{M}_j \mathbf{s}_j$, where $\mathbf{s}_j \in \mathbb{C}^{d_j}$ is the transmit signal of MT j , with $\mathbb{E}[\mathbf{s}_j] = \mathbf{0}$ and $\mathbb{E}[\mathbf{s}_j \mathbf{s}_j^H] = \mathbf{I}_{d_j}$, and $\mathbf{M}_j \in \mathbb{C}^{N_{\text{tx}} \times d_j}$ is the precoding matrix of MT j . The precoders satisfy the transmit power constraint $\text{tr}(\sum_{j=1}^J \mathbf{M}_j \mathbf{M}_j^H) = \rho$. In the multi-user setup, each MT reports its own feedback information k_j^* to the BS, which then jointly designs the precoders \mathbf{M}_j .

C. Pilot Transmission Phase

In the pilot transmission phase, each MT $j \in \mathcal{J}$ receives

$$\mathbf{Y}_j = \mathbf{H}_j \mathbf{P} + \mathbf{N}_j \in \mathbb{C}^{N_{\text{rx}} \times n_p} \quad (1)$$

where $\mathbf{N}_j = [\mathbf{n}'_{j,1}, \dots, \mathbf{n}'_{j,n_p}] \in \mathbb{C}^{N_{\text{rx}} \times n_p}$ with $\mathbf{n}'_{j,p} \sim \mathcal{N}_{\mathbb{C}}(\mathbf{0}, \sigma_j^2 \mathbf{I}_{N_{\text{rx}}})$, for $p \in \{1, 2, \dots, n_p\}$ and n_p is the number of pilots. It is assumed that the BS employs a uniform rectangular array (URA), so that the pilot matrix is a 2D-DFT (sub)matrix, constructed by the Kronecker product of two discrete Fourier transform (DFT) matrices, cf., e.g., [7]. To fulfill the power constraint each column \mathbf{p}_p of \mathbf{P} is normalized: $\|\mathbf{p}_p\|^2 = \rho$. In this work, we consider $n_p \leq N_{\text{tx}}$. For what follows, it is convenient to vectorize (1): $\mathbf{y}_j = \mathbf{A}\mathbf{h}_j + \mathbf{n}_j$, with the definitions $\mathbf{h}_j = \text{vec}(\mathbf{H}_j)$, $\mathbf{y}_j = \text{vec}(\mathbf{Y}_j)$, $\mathbf{n}_j = \text{vec}(\mathbf{N}_j)$, $\mathbf{A} = \mathbf{P}^T \otimes \mathbf{I}_{N_{\text{rx}}}$ and $\mathbf{n}_j \sim \mathcal{N}_{\mathbb{C}}(\mathbf{0}, \Sigma)$ with $\Sigma = \sigma_n^2 \mathbf{I}_{N_{\text{rx}} n_p}$. In case of a point-to-point MIMO system we drop the index j for notational convenience and end up with

$$\mathbf{y} = \mathbf{A}\mathbf{h} + \mathbf{n} \in \mathbb{C}^{N_{\text{rx}} n_p}. \quad (2)$$

For the ease of notation we use the channel matrix \mathbf{H} and its vectorized expression \mathbf{h} interchangeably in the following.

D. Channel Model and Data Generation

The QuaDRiGa channel simulator is used to generate a training dataset

$$\mathcal{H} = \{\mathbf{h}_\ell = \text{vec}(\mathbf{H}_\ell)\}_{\ell=1}^L \quad (3)$$

consisting of L channel realizations for the above system model. Since we utilize the same simulation setup, we refer the reader to [7] for more details.

III. GMM-BASED LIMITED FEEDBACK SCHEME

A. GMM Preliminaries

A GMM is a probability density function (PDF) of the form

$$f_h^{(K)}(\mathbf{h}) = \sum_{k=1}^K \pi_k \mathcal{N}_{\mathbb{C}}(\mathbf{h}; \boldsymbol{\mu}_k, \mathbf{C}_k) \quad (4)$$

where every summand is one of its K components. Maximum likelihood estimates of the parameters of a GMM, i.e., the mixing coefficients π_k , the means $\boldsymbol{\mu}_k$, and the covariances \mathbf{C}_k , can be computed using a training dataset \mathcal{H} , see (3), and an expectation maximization (EM) algorithm, see [18, Subsec. 9.2.2]. GMMs allow for the evaluation of *responsibilities* [18, Sec. 9.2]:

$$p(k \mid \mathbf{h}) = \frac{\pi_k \mathcal{N}_{\mathbb{C}}(\mathbf{h}; \boldsymbol{\mu}_k, \mathbf{C}_k)}{\sum_{i=1}^K p(i) \mathcal{N}_{\mathbb{C}}(\mathbf{h}; \boldsymbol{\mu}_i, \mathbf{C}_i)} \quad (5)$$

which correspond to the probability that a given \mathbf{h} stems from component k . Due to the joint Gaussianity of each GMM component and the AWGN, the GMM of the observations is straightforwardly computed using the GMM from (4) as

$$f_{\mathbf{y}}^{(K)}(\mathbf{y}) = \sum_{k=1}^K \pi_k \mathcal{N}_{\mathbb{C}}(\mathbf{y}; \mathbf{A}\boldsymbol{\mu}_k, \mathbf{A}\mathbf{C}_k\mathbf{A}^H + \Sigma). \quad (6)$$

Analogously, we can compute:

$$p(k \mid \mathbf{y}) = \frac{\pi_k \mathcal{N}_{\mathbb{C}}(\mathbf{y}; \mathbf{A}\boldsymbol{\mu}_k, \mathbf{A}\mathbf{C}_k\mathbf{A}^H + \Sigma)}{\sum_{i=1}^K \pi_i \mathcal{N}_{\mathbb{C}}(\mathbf{y}; \mathbf{A}\boldsymbol{\mu}_i, \mathbf{A}\mathbf{C}_i\mathbf{A}^H + \Sigma)}. \quad (7)$$

B. Point-to-Point MIMO System

In an offline phase, firstly, a codebook $\mathcal{Q} = \{\mathbf{Q}_k\}_{k=1}^K$, with $K = 2^B$, is constructed based on the GMM $f_h^{(K)}$ from (4) that is learned from the dataset (3). Therefore, by utilizing the GMM, the training data are clustered according to their GMM responsibilities. That is, \mathcal{H} is partitioned into K disjoint sets

$$\mathcal{V}_k = \{\mathbf{h} \in \mathcal{H} \mid p(k \mid \mathbf{h}) \geq p(j \mid \mathbf{h}) \text{ for } k \neq j\} \quad (8)$$

for $k = 1, \dots, K$. Then each codebook entry is determined:

$$\begin{aligned} \mathbf{Q}_k &= \arg \max_{\mathbf{Q} \succeq \mathbf{0}} \frac{1}{|\mathcal{V}_k|} \sum_{\text{vec}(\mathbf{H}) \in \mathcal{V}_k} r(\mathbf{H}, \mathbf{Q}) \\ \text{subject to } \text{tr}(\mathbf{Q}) &\leq \rho \end{aligned} \quad (9)$$

where the spectral efficiency is

$$r(\mathbf{H}, \mathbf{Q}) = \log_2 \det \left(\mathbf{I} + \frac{1}{\sigma_n^2} \mathbf{H} \mathbf{Q} \mathbf{H}^H \right). \quad (10)$$

This optimization problem is solved via a projected gradient ascent algorithm, cf. [7]. In the online phase, explicit channel estimation is bypassed and the feedback index is determined using the pilot observation \mathbf{y} :

$$k^* = \arg \max_k p(k \mid \mathbf{y}). \quad (11)$$

Obtaining the feedback using the GMM via (11) has a complexity of $\mathcal{O}(K N_{\text{rx}}^2 n_p^2)$, cf. [7]. Thus, the complexity does not scale with N_{tx} , which is particularly beneficial for massive MIMO systems. Note, that parallelization is possible, since all of the K responsibilities can be evaluated independently. The MT only requires the parameters of the GMM to compute

(11) and the knowledge of the codebook at the MT is not required. Moreover, the GMM of the observations, see (6), can be straightforwardly adapted at the MT to any SNR and pilot configuration, by simply updating the means and covariances, cf. (6), without retraining. As a baseline for the performance analysis perfect channel state information (CSI) can be used to determine the feedback

$$k^* = \arg \max_k p(k | \mathbf{h}). \quad (12)$$

C. Multi-User MIMO System

In [7] it was shown, that directional information of each codebook entry can be extracted by performing a singular value decomposition (SVD) of each transmit covariance matrix, i.e., $\mathbf{Q}_k = \mathbf{X}_k \mathbf{T}_k \mathbf{X}_k^H$, where \mathbf{T}_k contains the singular values in descending order, and taking the matrix $\bar{\mathbf{X}}_k$ which collects the first N_{rx} vectors of \mathbf{X}_k , as the respective directional information. Accordingly, $\mathcal{Q} = \{\bar{\mathbf{X}}_1, \bar{\mathbf{X}}_2, \dots, \bar{\mathbf{X}}_K\}$ constitutes a directional codebook, cf. [7]. Using the GMM-based approach each MT determines its feedback simply by:

$$k_j^* = \arg \max_k p(k | \mathbf{y}_j). \quad (13)$$

Each MT reports k_j^* to the BS which then represents each MT's channel by the subspace information associated with the respective codebook entry $\tilde{\mathbf{H}}_j = \bar{\mathbf{X}}_{k_j^*}^H$. The BS can then employ common precoding algorithms, such as the iterative weighted minimum mean square error (WMMSE) [19], in order to jointly design the precoders, cf. [7].

Alternatively, a generative modeling-based method was also proposed in [7]. The channel matrix of each MT may be modeled as a random variable, and the precoders are designed exploiting the stochastic WMMSE (SWMMSE) algorithm [20]. The GMM-based approach is able to generate samples following the channel's distribution due to the GMM's sample generation ability. Particularly, given the feedback k_j^* of each MT, see (13), one can draw samples via $\mathbf{h}_{j,\text{sample}} \sim \mathcal{N}_{\mathbb{C}}(\boldsymbol{\mu}_{k_j^*}, \mathbf{C}_{k_j^*})$, which represents statistical information about the channel of MT j . By utilizing the SWMMSE algorithm, the BS can design the precoders using the generated samples, cf. [7].

IV. ENABLING VARIABLE BIT LENGTHS

In this Section, we discuss how the GMM-based feedback scheme can be enabled to utilize variable bit lengths by only requiring a single GMM of a certain size, of which GMMs with a smaller number of components can be obtained. We investigate two different mixture reduction techniques, where given a GMM with $K = 2^B$ components, another GMM with fewer components $K_S = 2^{B_S}$, with, $K_S < K$, can be obtained.

There exist many methods to obtain a GMM with fewer components starting from a GMM with more components. In this work, we analyze two types of mixture reduction techniques. In particular, we use one *merging* strategy which

Algorithm 1 Variable Bit Lengths Enabled Through Merging.

Require: GMM with $K = 2^B$ components. Desired number of components $K_S = 2^{B_S}$ with $K_S < K$.

- 1: $i = K$ {track number of GMM components}
- 2: **repeat**
- 3: Calc. moment preserving merge of all pairs of components using (14).
- 4: Find pair with smallest dissimilarity $d_{a,b}$, via (15).
- 5: Replace this pair by their moment preserving merge.
- 6: $i \leftarrow i - 1$
- 7: **until** $i = K_S$
- 8: Partition \mathcal{H} into K_S disjoint sets \mathcal{V}_k with $k = 1, \dots, K_S$ according to the GMM responsibilities, cf. (8).
- 9: Compute codebook $\mathcal{Q} = \{\mathbf{Q}_k\}_{k=1}^{K_S}$ by solving (9) for each entry.

Algorithm 2 Variable Bit Lengths Enabled Through Pruning.

Require: GMM with $K = 2^B$ components. Desired number of components $K_S = 2^{B_S}$ with $K_S < K$.

- 1: Remove the $K - K_S$ components with smallest mixing coefficients π_k .
- 2: Re-normalize remaining mixing coefficients to one.
- 3: Discard codebook entries correspondingly and obtain $\mathcal{Q} = \{\mathbf{Q}_k\}_{k=1}^{K_S}$.

successively combines pairs of components with high similarity [17] and one *pruning* strategy, which simply discards components with a low contribution to the overall mixture [21].

In this work, we focus our analysis on the merging technique from [17]. Thereby, one replaces two mixture components with the smallest dissimilarity denoted by $\{\pi_a, \boldsymbol{\mu}_a, \mathbf{C}_a\}$ and $\{\pi_b, \boldsymbol{\mu}_b, \mathbf{C}_b\}$, by their moment preserving merge $\{\pi_m, \boldsymbol{\mu}_m, \mathbf{C}_m\}$ [17]:

$$\begin{aligned} \pi_m &= \pi_a + \pi_b \\ \boldsymbol{\mu}_m &= \frac{1}{\pi_m}(\pi_a \boldsymbol{\mu}_a + \pi_b \boldsymbol{\mu}_b) \\ \mathbf{C}_m &= \left(\frac{\pi_a}{\pi_m} \mathbf{C}_a + \frac{\pi_b}{\pi_m} \mathbf{C}_b + \frac{\pi_a \pi_b}{\pi_m^2} (\boldsymbol{\mu}_a - \boldsymbol{\mu}_b)(\boldsymbol{\mu}_a - \boldsymbol{\mu}_b)^H \right) \end{aligned} \quad (14)$$

The dissimilarity between two components is measured by

$$d_{a,b} = \frac{1}{2}[\pi_m \log \det(\mathbf{C}_m) - \pi_a \log \det(\mathbf{C}_a) - \pi_b \log \det(\mathbf{C}_b)] \quad (15)$$

which is an upper bound on the Kullback-Leibler divergence between the GMMs before and after the merge, cf. [17]. The merging procedure is successively repeated until a GMM of the desired size is obtained, i.e., when the number of GMM components is reduced to 2^{B_S} . After a GMM of the desired size is obtained, the corresponding codebook needs to be constructed at the BS in the same way as described in Section III-B. Algorithm 1 summarizes the merging procedure and the accompanying codebook construction.

The pruning strategy simply removes $K - K_S$ components with the smallest mixing coefficient π_k (see (4)), and the mixing coefficients of the remaining components are re-normalized to one [21]. A main advantage of the pruning strategy is its low computational complexity. In particular, it only requires traversing a list of sorted mixing coefficients. In this case, an updated codebook $\mathcal{Q} = \{\mathbf{Q}_k\}_{k=1}^{K_S}$ can simply be obtained by discarding the respective codebook entries which correspond to the removed GMM components. Algorithm 2 summarizes the pruning procedure.

Name	Covariance Parameters	Example
Full	$\frac{1}{2}KN(N+1)$	$8.4 \cdot 10^6$
Kronecker	$\frac{1}{2}K_{\text{rx}}N_{\text{rx}}(N_{\text{rx}}+1) + \frac{1}{2}K_{\text{tx}}N_{\text{tx}}(N_{\text{tx}}+1)$	$9.0 \cdot 10^3$
Toeplitz	$2K_{\text{rx}}N_{\text{rx}} + 4K_{\text{tx}}N_{\text{tx}}$	$2.1 \cdot 10^3$
Circulant	$K_{\text{rx}}N_{\text{rx}} + K_{\text{tx}}N_{\text{tx}}$	$5.7 \cdot 10^2$

TABLE I: Analysis of the number of parameters of the (structured) GMM.

V. REDUCING THE OFFLOADING OVERHEAD

To enable a MT to compute feedback indices via (11), the parameters of the GMM need to be offloaded to the MT upon entering the BS' coverage area, cf. [7]. To reduce the offloading overhead model-based insights can be utilized to obtain structured covariances with a lower number of parameters. For example, one can constrain the GMM covariances to a Kronecker factorization of the form $\mathbf{C}_k = \mathbf{C}_{\text{tx},k} \otimes \mathbf{C}_{\text{rx},k}$ which is shown to have no notable impact on the performance, [7], [9]. That is, instead of fitting a single unconstrained GMM with $N \times N$ -dimensional covariances, a transmit-side (receive-side) GMM with $N_{\text{tx}} \times N_{\text{tx}}$ ($N_{\text{rx}} \times N_{\text{rx}}$)-dimensional covariances and K_{tx} (K_{rx}) components is fitted. Afterwards, a $K = K_{\text{tx}}K_{\text{rx}}$ -components GMM with $N \times N$ -dimensional covariances is obtained by combinatorially computing all Kronecker products of the respective transmit- and receive-side covariance matrices.

In this work, we investigate the incorporation of further structural features to the transmit- and receive-side GMM covariance matrices imposed by the antenna structure at the transmitter or the receiver. In case of a uniform linear array (ULA), it is common to assume a Toeplitz covariance matrix, which for a large number of antenna elements, is well approximated by a circulant matrix, cf., e.g., [12]. If a URA is deployed, the structural assumptions result in block-Toeplitz matrices with Toeplitz blocks, or block-circulant matrices with circulant blocks, respectively [12].

In the assumed case of a URA employed at the BS with $N_{\text{tx},v}$ vertical and $N_{\text{tx},h}$ horizontal ($N_{\text{tx}} = N_{\text{tx},v}N_{\text{tx},h}$) elements, the structured covariances can be expressed as $\mathbf{C}_{\text{tx},k} = \mathbf{D}^H \text{diag}(\mathbf{c}_{\text{tx},k}) \mathbf{D}$, where on the one hand, when assuming a Toeplitz structure, $\mathbf{D} = \mathbf{D}_{N_{\text{tx},v}} \otimes \mathbf{D}_{N_{\text{tx},h}}$, where \mathbf{D}_T contains the first T columns of a $2T \times 2T$ DFT matrix, and $\mathbf{c}_{\text{tx},k} \in \mathbb{R}_+^{4N_{\text{tx}}}$ [11], [12]. On the other hand, when assuming circular structure, we have $\mathbf{D} = \mathbf{F}_{N_{\text{tx},v}} \otimes \mathbf{F}_{N_{\text{tx},h}}$, where \mathbf{F}_T is the $T \times T$ DFT-matrix, and $\mathbf{c}_{\text{tx},k} \in \mathbb{R}_+^{N_{\text{tx}}}$. At the MTs, we assume to have ULAs, thus \mathbf{D} contains either the first N_{rx} columns of a $2N_{\text{rx}} \times 2N_{\text{rx}}$ DFT matrix and correspondingly $\mathbf{c}_{\text{rx},k} \in \mathbb{R}_+^{2N_{\text{rx}}}$ (Toeplitz), or $\mathbf{D} = \mathbf{F}_{N_{\text{rx}}}$ and $\mathbf{c}_{\text{rx},k} \in \mathbb{R}_+^{N_{\text{rx}}}$ (circulant). With these structural constraints the GMM covariances are fully determined by the vectors $\mathbf{c}_{\{\text{tx},\text{rx}\},k}$. Overall, these insights drastically reduce the offloading overhead, allow for a lower offline training complexity, help to parallelize the fitting process, and require fewer training samples since fewer parameters need to be learned, cf. [11], [12].

Table I illustrates exemplarily the difference in the number of GMM covariance parameters (taking symmetries into ac-

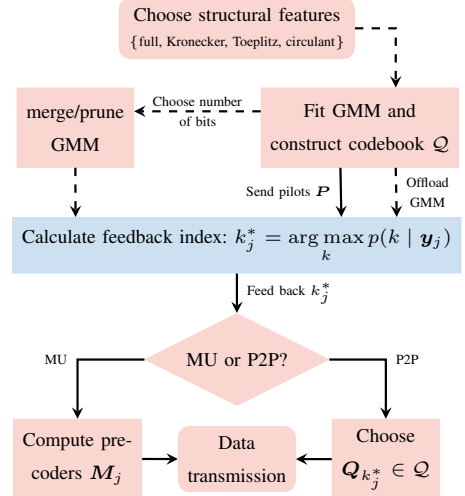


Fig. 1: Flowchart of the improved versatile feedback scheme. Red (blue) colored nodes are processed at the BS (MTs) and solid (dashed) arrows indicate online (offline) processing.

count), where we plug in the simulation parameters of one of the settings with $B = 6$, $(N_{\text{tx}}, N_{\text{rx}}) = (32, 16)$, and $(K_{\text{tx}}, K_{\text{rx}}) = (16, 4)$, which we consider in Section VII. We can see that, the structural constraints drastically reduce the offloading overhead.

VI. DISCUSSION ON THE ENHANCED VERSATILITY

The low-complexity GMM-based feedback scheme from [7] exhibits great flexibility with respect to the transmission mode, i.e., either point-to-point MIMO or MU-MIMO, the supported SNR range, the number of pilots, and the choice of the precoding algorithm, but utilizes a GMM with a predefined number of components $K = 2^B$. In principle, the BS could offload many GMMs with different sizes, which would allow for different numbers of feedback bits. However, the corresponding signaling overhead might be unaffordable in practice. Therefore, in Section IV we discussed different mixture reduction techniques and their corresponding codebook update procedures. Particularly, given a GMM with $K = 2^B$ components, GMMs with fewer components $K_S = 2^{B_S}$, i.e., $K_S < K$, can be obtained. Accordingly, the scheme is enabled to support variable bit lengths by successively decreasing the number of components and thereby the number of feedback bits starting from B bits ($B-1, B-2, \dots$). Due to the simplicity of the pruning strategy, it can be straightforwardly implemented at the MTs. The merging strategy can be either conducted at the MTs, or to reduce their computational burden, the BS could offload additional lists with the respective merging updates. Moreover, the MT only requires the GMM and does not need to be aware of the codebook in order to compute the feedback via (11). Altogether, this allows for variable feedback bit lengths and eliminates the necessity of offloading a particularly trained GMM for different feedback bit lengths and thereby improves the versatility of the feedback scheme. Additionally, in Section V we discussed how model-based insights can help

to effectively reduce the offloading overhead. Fig. 1 provides a flowchart of the enhanced GMM-based feedback scheme.

VII. SIMULATION RESULTS

We generate datasets for both, the UL and DL domain of the scenario described in Section II-D: \mathcal{H}^{UL} and \mathcal{H}^{DL} . The GMM is fitted centrally at the BS using the training set $\mathcal{H} = \mathcal{H}^{\text{UL}}$ which consists of $L = 20 \cdot 10^3$ samples, cf., [5], [7], [13]–[15]. The following transmit strategies are always evaluated in the DL domain using \mathcal{H}^{DL} , comprised of $L = 10 \cdot 10^3$ channels. The data samples are normalized such that $\mathbb{E}[\|\mathbf{h}\|^2] = N = N_{\text{tx}}N_{\text{rx}}$. We further set $\rho = 1$ which allows to define the SNR as $\frac{1}{\sigma_n^2}$ for all MTs, i.e., when $\sigma_j^2 = \sigma_n^2, \forall j \in \mathcal{J}$.

In the single-user case, we will compare to codebook based approaches utilizing Lloyd’s clustering algorithm, cf. [3], [7]. In case of MU-MIMO systems, we will either use directional information extracted from the Lloyd codebooks or we will use the random codebook approach, cf. [2], [7]. With these approaches, prior to codebook entry selection, the channel needs to be estimated. To this end, we consider three different channel estimators, which are briefly explained in the following. The recently proposed GMM-based channel estimator \hat{h}_{GMM} , from [9] is one of them and utilizes the same GMM as found in Section III and calculates a convex combination of per-component linear minimum mean square error (LMMSE) estimates, cf. [7], [9]. This estimator is proven to asymptotically converge to the optimal conditional mean estimator as the number of components K is increased, cf. [9]. Another baseline is the LMMSE estimator \hat{h}_{LMMSE} , where the sample covariance matrix is constructed given the set \mathcal{H} , cf. [7], [9], [15]. Lastly, we consider a compressive sensing channel estimation approach \hat{h}_{OMP} which utilizes the orthogonal matching pursuit (OMP) algorithm, cf. [7], [22].

A. Point-to-point MIMO

We depict the normalized spectral efficiency (nSE) as performance measure, where the spectral efficiency achieved with a certain transmit strategy is normalized by the optimal water-filling solution, cf. [1]. The empirical complementary cumulative distribution function (cCDF) $P(\text{nSE} > s)$ of the normalized spectral efficiency, corresponds to the empirical probability that nSE exceeds a specific value s .

In Fig. 2, we denote by “Setup A” a system with $N_{\text{tx}} = 32$ ($N_{\text{tx,h}} = 8, N_{\text{tx,v}} = 4$), $N_{\text{rx}} = 16$, and SNR = 10 dB, and with “Setup B” a system with $N_{\text{tx}} = 16$ ($N_{\text{tx,h}} = 4, N_{\text{tx,v}} = 4$), $N_{\text{rx}} = 4$, and SNR = 0 dB. In the following, we consider the Kronecker GMM (“kGMM”) with full transmit- and receive-side GMMs and assume perfect CSI, i.e., the feedback information is determined via (12). For “Setup A” we fit a GMM with $K = 256$ ($B = 8, K_{\text{tx}} = 32$, and $K_{\text{rx}} = 8$) components and first reduce to a GMM with $K_{S_1} = 64$ ($B_{S_1} = 6$) components and continue the reduction to another one with $K_{S_2} = 8$ ($B_{S_2} = 3$) components, by either applying the merging strategy (“mkGMM”) or the pruning strategy (“pkGMM”). Moreover, with “kGMM” we denote the case of directly fitting a GMM with 64 ($B = 6, K_{\text{tx}} = 16$,

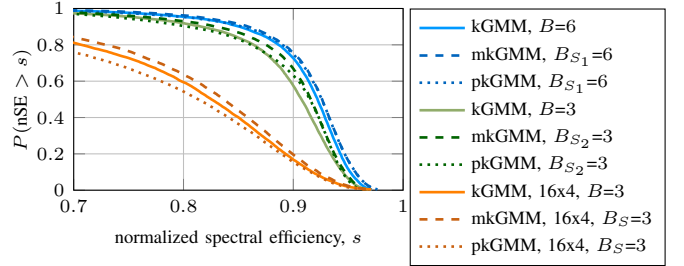


Fig. 2: Empirical cCDFs of the normalized spectral efficiencies for two setups using either mixture reduction techniques or the direct fitting approach **assuming perfect CSI**. Setup A: $N_{\text{tx}} = 32$ ($N_{\text{tx,h}} = 8, N_{\text{tx,v}} = 4$), $N_{\text{rx}} = 16$, and SNR = 10 dB. Setup B: $N_{\text{tx}} = 16$ ($N_{\text{tx,h}} = 4, N_{\text{tx,v}} = 4$), $N_{\text{rx}} = 4$, and SNR = 0 dB.

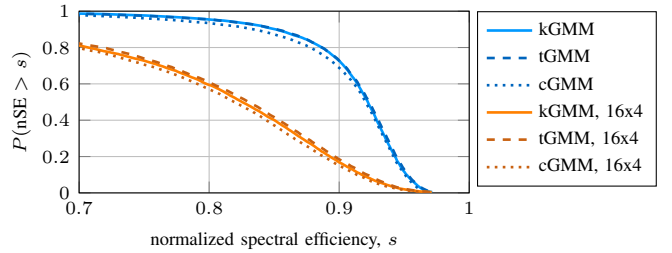


Fig. 3: Empirical cCDFs of the normalized spectral efficiencies for two setups using differently structured GMMs **assuming perfect CSI**. Setup A: $N_{\text{tx}} = 32$ ($N_{\text{tx,h}} = 8, N_{\text{tx,v}} = 4$), $N_{\text{rx}} = 16$, and SNR = 10 dB, with $B = 6$. Setup B: $N_{\text{tx}} = 16$ ($N_{\text{tx,h}} = 4, N_{\text{tx,v}} = 4$), $N_{\text{rx}} = 4$, and SNR = 0 dB, with $B = 3$.

and $K_{\text{rx}} = 4$), or with 8 ($B = 3, K_{\text{tx}} = 4$, and $K_{\text{rx}} = 2$) components. We can observe, that both mixture reduction approaches not only enable the feedback scheme with variable bit lengths, but at the same time provide at least a similar performance as the respective direct fitting approaches. In case of “Setup B”, we fit a GMM with $K = 256$ components and reduce to one with $K_S = 8$ ($B_S = 3$) components and compare to a GMM directly fitted with 8 ($K_{\text{tx}} = 4$, and $K_{\text{rx}} = 2$) components. In this setup, the merging strategy performs best, whereas the low-complexity pruning strategy yields a slightly worse performance as compared to the direct fitting approach. Altogether, the applied mixture reduction techniques enable variable bit lengths and in some cases even improve the performance as a consequence of the enhanced clustering ability, cf. [16].

In Fig. 3, consider the same two setups and denote by “tGMM” or “cGMM” Kronecker GMMs constructed by (block) Toeplitz or (block) circulant transmit- and receive-side GMMs, respectively, with 64 components ($B = 6, K_{\text{tx}} = 16$, and $K_{\text{rx}} = 4$) in case of “Setup A”, and 8 components ($B = 3, K_{\text{tx}} = 4$, and $K_{\text{rx}} = 2$) in case of “Setup B”. We can observe, that although the Toeplitz approximation (“tGMM”) drastically reduces the offloading overhead, it achieves the same performance as the Kronecker GMM with full transmit- and receive-side GMMs (“kGMM”). The circulant approximation (“cGMM”) with even less offloading overhead, slightly degrades the performance.

However, assuming perfect CSI at the MT in the online

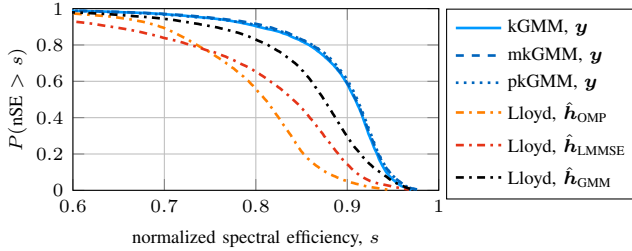


Fig. 4: Empirical cCDFs of the normalized spectral efficiencies using either mixture reduction techniques ($B = 8$ to $B_S = 6$) or the direct fitting approach ($B = 6$) for a system with $N_{tx} = 32$, $N_{rx} = 16$, SNR = 15 dB, and $n_p = 4$ pilots.

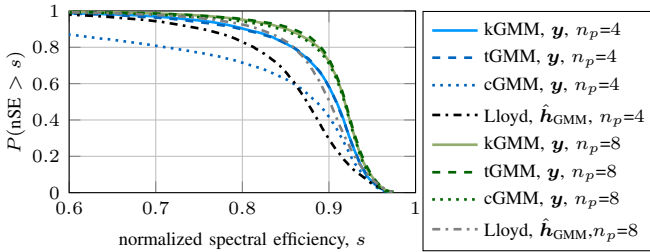


Fig. 5: Empirical cCDFs of the normalized spectral efficiencies using differently structured GMMs for a system with $N_{tx} = 32$, $N_{rx} = 16$, SNR = 15 dB, different number of pilots n_p , and $B = 6$ bits.

phase is not feasible. In the following, we consider imperfect CSI, i.e., systems with reduced pilot overhead ($n_p \leq N_{tx}$). With “Lloyd, $\{\hat{h}_{GMM}, \hat{h}_{OMP}, \hat{h}_{LMMSE}\}$ ” we depict the conventional approaches which first estimate the channel and then determine the feedback information, cf. [7]. To be fair, in the remainder, the conventional approaches always utilize the same number of feedback bits of interested, i.e., B_S bits if merging or pruning is considered, or B bits if not.

In Fig. 4, we simulate a setup with $N_{tx} = 32$ ($N_{tx,h} = 8, N_{tx,v} = 4$), $N_{rx} = 16$, SNR = 15 dB, and $n_p = 4$ pilots. We again consider a GMM with $K = 256$ ($B = 8$, $K_{tx} = 32$, and $K_{rx} = 8$) components and reduce to a GMM with $K_S = 64$ ($B_S = 6$) components, by applying the merging strategy (“mkGMM”) or the pruning strategy (“pkGMM”). We can observe, that the GMM-based feedback approach (“kGMM, y ”), which circumvents explicit channel estimation, is superior as compared to the baselines and provides a higher robustness against CSI imperfections. The proposed merging and pruning strategies exhibit a similar robustness.

In Fig. 5, we have $N_{tx} = 32$ ($N_{tx,h} = 8, N_{tx,v} = 4$), $N_{rx} = 16$, SNR = 15 dB, and $n_p \in \{4, 8\}$ pilots and depict differently structured GMMs with $K = 64$ ($K_{tx} = 16$, and $K_{rx} = 4$) components. The Toeplitz approximation (“tGMM”) with a reduced number of parameters achieves the same performance as compared to the Kronecker GMM with full transmit- and receive-side GMMs (“kGMM”), irrespective of the number of pilots. With $n_p = 4$, the proposed approach “tGMM” attains the same performance as the conventional Lloyd approach with twice as much pilots ($n_p = 8$). This shows, the great potential of the enhanced GMM-based feedback scheme in systems with reduced pilot overhead. Inter-

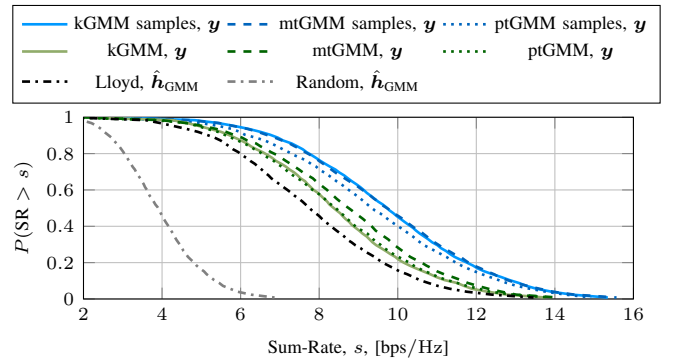


Fig. 6: Empirical cCDFs of the sum-rate using either mixture reduction techniques ($B = 8$ to $B_S = 6$) combined with Toeplitz structured GMMs or the direct fitting approach ($B = 8$) when the iterative WMMSE or the SWMMSE are employed, for a system with $N_{tx} = 16$, $N_{rx} = 4$, $J = 4$ MTs, SNR = 5 dB, and $n_p = 8$ pilots.

estingly, in case of the circulant approximation (“cGMM”) a performance degradation can be observed if $n_p = 4$. It seems that the expressivity of the circulant GMM with a very low number of parameters is too restrictive to be applied for systems with a few pilots only. Since the Toeplitz approach provides a higher robustness, we will restrict our further analysis to it in the remainder.

B. Multi-user MIMO

In the multi-user case, we depict the sum-rate as performance measure, cf. [7]. We depict the results for 2,500 constellations, where for each constellation, we draw J MTs randomly from our evaluation set \mathcal{H}^{DL} . The empirical cCDF $P(SR > s)$ of the sum-rate, is used to depict the empirical probability that the sum-rate (SR) exceeds a specific value s . Although the GMM-based feedback scheme can be used in combination with non-iterative precoding algorithms, in the following we restrict our analysis to the iterative WMMSE and to the SWMMSE in order to design the precoders, since the performance with these methods is generally better, cf. [7].

In the following, with “GMM, y ” we denote the cases, where the observations y_j are used at each MT j to determine a feedback index using the GMM feedback encoding approach, cf. (13). We omit the index j in the legend for notational convenience. The channel of each MT is then represented by the subspace information extracted from the GMM codebook, cf. Section III-C. With “{Lloyd, Random}, $\{\hat{h}_{GMM}, \hat{h}_{OMP}, \hat{h}_{LMMSE}\}$ ”, the channel is firstly estimated at each MT and then the feedback information is determined using either the directional Lloyd codebook or the random codebook approach, cf. [7]. These methods use the iterative WMMSE, cf. [19, Algorithm 1]. Additionally, with “GMM samples, y ”, we denote the case, where we generate samples which represent each MT’s distribution using the GMM and feed them to the SWMMSE algorithm, cf. Section III-C. In all iterative approaches, we set $I_{max} = 300$ iterations.

In the remainder, we combine both, the Toeplitz approximation and the mixture reduction techniques in a setup with $N_{tx} = 16$ ($N_{tx,h} = 4, N_{tx,v} = 4$) and $N_{rx} = 4$, and $J = 4$ users. In particular, we fit a Kronecker GMM constructed

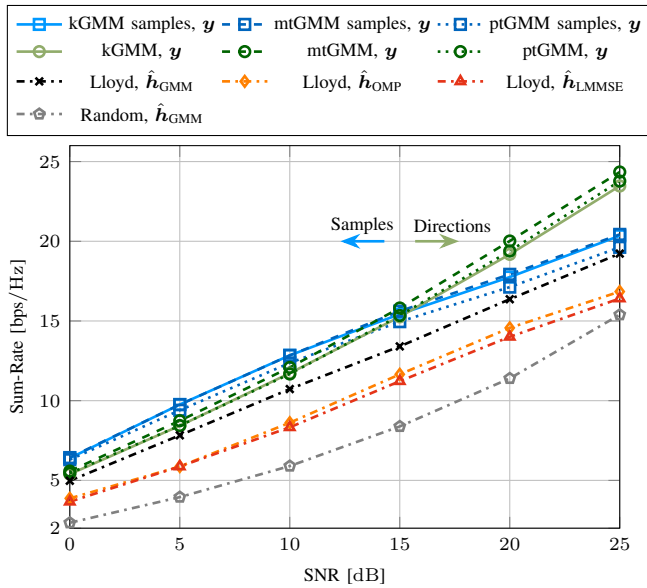


Fig. 7: The average sum-rate over the SNR using either mixture reduction techniques ($B = 8$ to $B_S = 6$) combined with Toeplitz structured GMMS or the direct fitting approach ($B = 6$) when the iterative WMMSE or the SWMMSE are employed, for a system with $N_{tx} = 16$, $N_{rx} = 4$, $J = 4$ MTs, and $n_p = 8$ pilots.

by (block) Toeplitz transmit- and receive-side GMMS, with $K = 256$ components and reduce to a GMM with $K_S = 64$ ($B_S = 6$) components denoted by “mtGMM” and “ptGMM”, and compare to a GMM directly fitted with 64 ($K_{tx} = 16$, and $K_{rx} = 4$) components with full transmit- and receive-side GMMS (“kGMM”). In Fig. 6, with $\text{SNR} = 5$ dB and $n_p = 8$ pilots, we can see that the pruning and merging strategy in combination with the Toeplitz structured covariances in case of the directional (subspace) approach, i.e., “ptGMM, y ” and “mtGMM, y ”, perform similarly or even better than the “kGMM, y ” and outperform the conventional methods “{Lloyd, Random}, \hat{h}_{GMM} ”, by far. With the generative modeling approach, the merging method “mtGMM samples, y ” performs equally well as “kGMM samples, y ”, whereas the pruning method “ptGMM samples, y ” performs slightly worse.

A similar behaviour is present in Fig. 7, where we still consider the same setting with $n_p = 8$ pilots, but vary the SNR and depict the sum-rate averaged over all constellations. Interestingly, with an increasing SNR, the gap between “mtGMM, y ” and “kGMM, y ” increases. Similarly, the gap between “ptGMM samples, y ” and “kGMM samples, y ” increases with larger SNR values. As reported in [7], jointly designing the precoders by using the generative modeling approach is beneficial for low to medium SNR values, and for larger SNR values the directional approach is superior. This property can be similarly observed if the merging or pruning procedures are applied, and is illustrated by the arrows in Fig. 7. Altogether, the enhanced GMM-based feedback scheme outperforms the baselines in a multi-user system with reduced pilot overhead.

VIII. CONCLUSION

In this work, we enhanced the versatile GMM-based feedback from [7] scheme by enabling variable bit lengths and

incorporating further model-based structural constraints with the goal to reduce the offloading overhead. To this end, we analyzed two mixture reduction techniques, i.e., one pruning and one merging strategy and found out, that both approaches enable the scheme with variable bit lengths and allow for a trade-off between complexity and performance. Moreover, numerical results showed the remarkable performance of the combination of mixture reduction techniques together with structured GMMS.

REFERENCES

- [1] D. J. Love, R. W. Heath, V. K. N. Lau, D. Gesbert, B. D. Rao, and M. Andrews, “An overview of limited feedback in wireless communication systems,” *IEEE J. Sel. Areas Commun.*, vol. 26, no. 8, pp. 1341–1365, 2008.
- [2] N. Ravindran and N. Jindal, “Limited feedback-based block diagonalization for the MIMO broadcast channel,” *IEEE J. Sel. Areas Commun.*, vol. 26, no. 8, pp. 1473–1482, 2008.
- [3] V. Lau, Y. Liu, and T.-A. Chen, “On the design of MIMO block-fading channels with feedback-link capacity constraint,” *IEEE Trans. Commun.*, vol. 52, no. 1, pp. 62–70, 2004.
- [4] J. Jang, H. Lee, I.-M. Kim, and I. Lee, “Deep learning for multi-user MIMO systems: Joint design of pilot, limited feedback, and precoding,” *IEEE Trans. Commun.*, vol. 70, no. 11, pp. 7279–7293, 2022.
- [5] N. Turan, M. Koller, S. Bazzi, W. Xu, and W. Utschick, “Unsupervised learning of adaptive codebooks for deep feedback encoding in FDD systems,” in *55th Asilomar Conf. Signals, Syst., Comput.*, 2021, pp. 1464–1469.
- [6] N. Turan, M. Koller, B. Fesl, S. Bazzi, W. Xu, and W. Utschick, “GMM-based codebook construction and feedback encoding in FDD systems,” in *56th Asilomar Conf. Signals, Syst., Comput.*, 2022, pp. 37–42.
- [7] N. Turan, B. Fesl, M. Koller, M. Joham, and W. Utschick, “A versatile low-complexity feedback scheme for FDD systems via generative modeling,” 2023, arXiv preprint: 2304.14373.
- [8] T. T. Nguyen, H. D. Nguyen, F. Chamroukhi, and G. J. McLachlan, “Approximation by finite mixtures of continuous density functions that vanish at infinity,” *Cogent Math. Statist.*, vol. 7, no. 1, p. 1750861, 2020.
- [9] M. Koller, B. Fesl, N. Turan, and W. Utschick, “An asymptotically MSE-optimal estimator based on Gaussian mixture models,” *IEEE Trans. Signal Process.*, vol. 70, pp. 4109–4123, 2022.
- [10] B. Fesl, N. Turan, M. Joham, and W. Utschick, “Learning a Gaussian mixture model from imperfect training data for robust channel estimation,” *IEEE Wireless Commun. Lett.*, 2023.
- [11] B. Fesl, M. Joham, S. Hu, M. Koller, N. Turan, and W. Utschick, “Channel estimation based on Gaussian mixture models with structured covariances,” in *56th Asilomar Conf. Signals, Syst., Comput.*, 2022, pp. 533–537.
- [12] N. Turan, B. Fesl, M. Grundej, M. Koller, and W. Utschick, “Evaluation of a Gaussian mixture model-based channel estimator using measurement data,” in *Int. Symp. Wireless Commun. Syst. (ISWCS)*, 2022.
- [13] W. Utschick, V. Rizzello, M. Joham, Z. Ma, and L. Piazzoli, “Learning the CSI recovery in FDD systems,” *IEEE Trans. Wireless Commun.*, 2022.
- [14] N. Turan, M. Koller, V. Rizzello, B. Fesl, S. Bazzi, W. Xu, and W. Utschick, “On distributional invariances between downlink and uplink MIMO channels,” in *25th Int. ITG Workshop Smart Antennas (WSA)*, 2021.
- [15] B. Fesl, N. Turan, M. Koller, M. Joham, and W. Utschick, “Centralized learning of the distributed downlink channel estimators in FDD systems using uplink data,” in *25th Int. ITG Workshop Smart Antennas (WSA)*, 2021.
- [16] C. Hennig, “Methods for merging Gaussian mixture components,” *Adv. Data Anal. Classif.*, vol. 4, p. 3–34, 2010.
- [17] A. Runnalls, “Kullback-Leibler approach to Gaussian mixture reduction,” *IEEE Trans. Aerosp. Electron. Syst.*, vol. 43, no. 3, pp. 989–999, 2007.
- [18] C. M. Bishop, *Pattern Recognition and Machine Learning (Information Science and Statistics)*. Berlin, Heidelberg: Springer-Verlag, 2006.
- [19] Q. Hu, Y. Cai, Q. Shi, K. Xu, G. Yu, and Z. Ding, “Iterative algorithm induced deep-unfolding neural networks: Precoding design for multiuser MIMO systems,” *IEEE Trans. Wireless Commun.*, vol. 20, no. 2, pp. 1394–1410, 2021.

- [20] M. Razaviyayn, M. S. Boroujeni, and Z.-Q. Luo, “A stochastic weighted MMSE approach to sum rate maximization for a MIMO interference channel,” in *IEEE 14th Int. Workshop Signal Process. Adv. Wireless Commun. (SPAWC)*, 2013, pp. 325–329.
- [21] D. F. Crouse, P. Willett, K. Pattipati, and L. Svensson, “A look at Gaussian mixture reduction algorithms,” in *14th Int. Conf. Inf. Fusion*, 2011.
- [22] A. Alkhateeb, G. Leus, and R. W. Heath, “Compressed sensing based multi-user millimeter wave systems: How many measurements are needed?” in *IEEE Int. Conf. Acoust., Speech Signal Process. (ICASSP)*, 2015, pp. 2909–2913.